

Minimalist machine-learned interatomic potentials can predict complex structural behaviors accurately

Iñigo Robredo-Magro,¹ Binayak Mukherjee,¹ Hugo Aramberri,¹ and Jorge Íñiguez-González^{1,2}

¹*Smart Materials Unit, Luxembourg Institute of Science and Technology (LIST), Avenue des Hauts-Fourneaux 5, L-4362 Esch/Alzette, Luxembourg*

²*Department of Physics and Materials Science, University of Luxembourg, Rue du Brill 41, L-4422 Belvaux, Luxembourg*

The past decade has witnessed a spectacular development of machine-learned interatomic potentials (MLIPs), to the extent that they are already the approach of choice for most atomistic simulation studies not requiring an explicit treatment of electrons. Typical MLIP usage guidelines emphasize the need for exhaustive training sets and warn against applying the models to situations not considered in the corresponding training space. This restricts the scope of MLIPs to interpolative calculations, essentially denying the possibility of using them to discover new phenomena in a serendipitous way. While there are reasons to be cautious, here we adopt a more sanguine view and challenge the predictive power of two representative and widely available MLIP approaches. We work with minimalist training sets that rely on little prior knowledge of the investigated materials. We show that the resulting models – for which we adopt modest/default choices of the defining hyperparameters – are very successful in predicting non-trivial structural effects (competing polymorphs, energy barriers for structural transformations, occurrence of non-trivial topologies) in a way that is qualitatively and quasi-quantitatively correct. Our results thus suggest an expanded scope of modern MLIP approaches, evidencing that somewhat trivial – and easy to compute – models can be an effective tool for the discovery of novel and complex physical phenomena.

I. INTRODUCTION

Machine-learned force fields or interatomic potentials (MLFFs or MLIPs) have become an efficient tool for first-principles atomistic modeling.^{1–8} When trained on quantum-mechanical data, they can achieve near-first-principles accuracy at a small fraction of the cost. Most current applications of MLIPs rely on large, carefully selected training sets and optimized hyperparameters, with the aim of ensuring that the model interpolates within its training domain. This strategy minimizes errors and yields very accurate potentials. It also seems to imply that the scope of MLIPs is confined to regions of the configuration space explored in the training set.

Ferroelectric materials exhibit highly non-trivial structural and lattice-dynamical behavior driven by competing instabilities and strong anharmonic effects.^{9–12} Their phase diagrams often include multiple polymorphs with quasi-degenerate free energies, intricate transformation paths between phases, and complex topological features. Further, their properties are highly sensitive to electric and elastic boundary conditions, size, temperature, and external fields. First-principles methods, as those based on Density Functional Theory (DFT),^{13–15} can predict and explain such effects with high accuracy, but their computational cost limits their use in large-scale or long-time simulations. Successful partial solutions to this problem have been developed over the years, notably through the so-called “second-principles” methods^{16–19} and other first-principles-based effective potential approaches.^{20–29} Yet, such schemes lack generality, which limits the span of materials and effects investigated. For example: novel fluorite ferroelectrics such as hafnia, characterized by an intimate connection between ferroelectric switching and ionic mobility, are all

but impossible to treat within the traditional effective schemes. Modern MLIPs are expected to drastically improve this situation and become the approach of choice for simulations of ferroelectric and related phenomena. Symbiotically, ferroelectrics offer a stringent playground for testing the performance of modern ML approaches.

In this context, it is relevant to note that relatively simple second-principles potentials and effective Hamiltonians have been remarkably successful in *predicting* behaviors beyond the scope of the DFT data used to compute the model parameters. Notable examples include complex composition-driven phase transitions (as in the so-called “morphotropic phase boundary” of $\text{PbZr}_{1-x}\text{Ti}_x\text{O}_3$ solid solutions²⁴) or the occurrence of topological skyrmion-like quasiparticles in nanoferroelectrics.^{30–34} These and other striking discoveries – eventually confirmed experimentally – emerged serendipitously from the simulations. Can MLIPs deliver similarly unforeseen predictions, or are these the patrimony of relatively simple models that can be expected to yield meaningful results beyond their training space? This is a relevant question to define the application scope of MLIPs and to what extend resorting to simpler potentials may still be required in exploratory studies.

In this work we test the predictive performance of MLIPs for challenging ferroelectricity-related effects and provide an answer to the above question. We adopt a peculiar approach, whereby we *pretend* we know little about the materials at the time of constructing the models; thus, we use minimalist training sets of the type one would consider by default as a first step in the investigation of an all-new compound. Then, we test whether the MLIPs thus constructed are able to predict the non-trivial structural properties that we know these compounds display.

Specifically, we work with two widely available and representative MLIP types: the kernel-based Gaussian Approximation Potentials¹ (GAPs) implemented in the Vienna *ab initio* software package^{3,35,36} (VASP) and the equivariant deep learning potentials provided in Allegro.^{5,37,38} In both cases we adopt modest or default (when available) choices for the hyperparameters defining the MLIPs, which are supposed to strike a balance between accuracy and computational burden in the description of generic compounds. Also, we use the Bayesian “on-the-fly” approach implemented in VASP to derive training sets,³ using material-unspecific control parameters and starting the procedure from the experimentally well-known structural phases of the respective compounds. Following this minimalist spirit, we generate our training sets using small periodically-repeated supercells containing 40 atoms at most.

We apply this MLIP-construction approach to four representative ferroelectric and related compounds, namely BaTiO₃, BiFeO₃, PbZrO₃, and HfO₂. We find that our basic models successfully reproduce a variety of non-trivial behaviors, such as the vortex-antivortex electric-dipole lattice recently observed in BaTiO₃ moiré bilayers,³⁹ the non-trivial polarization switching path (and its corresponding energy barrier) in BiFeO₃,⁴⁰ the competition of polar and antipolar polymorphs in PbZrO₃,^{41,42} and the occurrence of a ferroelectric polymorph in HfO₂.⁴³ In all cases we find that the models predict the examined properties in a qualitatively correct way. Furthermore, our quantitative results – including tiny energy differences between competing polymorphs and polarization-switching energy barriers – turn out to be incredibly accurate in most cases.

The structure of the paper is as follows. In Section II we describe the construction of our minimalist MLIPs. In Section III we present the obtained models and how well they perform as regards both interpolating within the training set and extrapolating to unexplored space. In Section IV we further discuss the implications of this study. Finally, in Section V we summarize our main findings and conclusions.

II. MINIMALIST MODELS

The guiding principle of our modeling approach is simplicity and minimal prior knowledge. For all models considered in this work, we deliberately adopt a low-effort protocol: training sets are kept small and left at their default values; no optimization or manual tuning is performed at any stage. This strategy allows us to evaluate the intrinsic predictive capacity of modern MLIP frameworks under the most basic by-default fool-proof conditions. Our aim is not to benchmark best-case performance, but rather to assess how well these models can generalize when trained in a straightforward, out-of-the-box manner.

A. Kernel-based GAP interatomic potentials

We first consider a kernel-based interatomic potential trained using the Bayesian on-the-fly framework implemented in VASP.^{1,3} This method is rooted in kernel ridge regression, using Smooth Overlap of Atomic Positions (SOAP) descriptors⁴⁴ to represent local atomic environments and build GAPs that mimic DFT accuracy. Training data is gathered during relatively short first-principles molecular dynamics (MD) simulations of the studied systems.³ We train starting from well-known polymorphs of each of the compounds, running for 10000 steps of 2 fs, with a linear temperature ramp from 10 K to 300 K.

We set the model parameters to the default values of VASP: the cut-off radius for the radial descriptor is 8 Å (which roughly coincides with the lattice parameter used for the perovskite supercells), the cut-off radius for the angular descriptor is 5 Å (enough to include at least 20 nearest neighbors for each atom). The number of basis functions used to expand the radial and angular descriptors is set to 12 and 8, respectively, and the maximum angular momentum of spherical harmonics is set to 6. The threshold for error estimation is set to 0.002, with automatic updating to a value proportional to the average errors as implemented by default. As the simulation runs, the model learns in real time: in essence, new configurations are flagged if the predicted maximum Bayesian error is larger than a threshold, and a new first principles calculation is performed, adding it to the dataset. In the following, we refer to these models generically as “VASP MLIPs”.

B. E(3)-equivariant neural networks

We also constructed potentials based on the Allegro neural network architecture,^{5,37,38} trained using the very same dataset generated by the VASP on-the-fly procedure. Allegro is based on the same symmetry principles as the better-known NequIP scheme – specifically, E(3)-equivariance – but differs in how it processes atomic environments. Instead of relying on message passing between atoms, Allegro builds local representations directly from the fixed neighborhood of each atom, using a sequence of tensor products to capture many-body interactions. This design avoids the iterative communication steps typical of message-passing networks, leading to improved scalability and faster evaluation, particularly in large systems.

We make a reasonable choice of Allegro hyperparameters based on the documentation provided by the developers, with no effort to tune them. We set the radial cut-off to the same value as for the VASP MLIPs, 8 Å. For the rest of the parameters, we take them as in the application example proposed with Allegro. We use 2 tensor layers with full O(3) symmetry, polynomial cut-off of 6, and embed feature multiplicity of 64. We set the maximum order of spherical harmonics embedding to 3, which

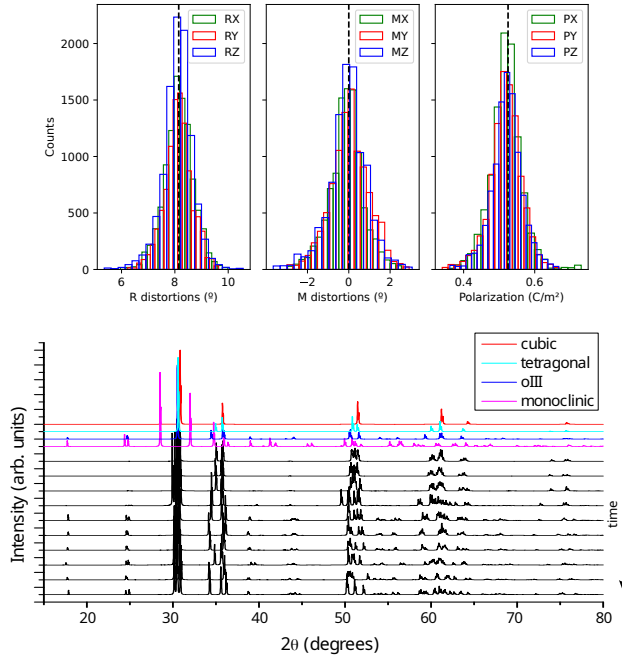


FIG. 1. Configuration space explored in the training of BiFeO_3 and HfO_2 . The top panels show histograms for the main perovskite distortions: antiphase (R) and in-phase (M) octahedral tilts, as well as the polarization (P). The histograms are derived from the MD trajectories corresponding to the on-the-fly training starting from the ferroelectric ground state ($R3c$ polymorphs); they show that the material fluctuates around the ground state configuration, characterized by $R_x = R_y = R_z \neq 0$, $P_x = P_y = P_z \neq 0$, and $M_x = M_y = M_z = 0$ (values indicated by dashed black lines). The bottom panel shows simulated diffraction patterns for configurations visited during the HfO_2 training, corresponding to the MD run that started from the tetragonal polymorph. By comparison with reference data (colored) for important HfO_2 phases, we can appreciate that the material evolved spontaneously toward low-symmetry polymorphs during the MD run, visiting the oIII ferroelectric phase in particular.

is the recommended value for more accurate MLIPs while being slower. We train on energies, forces, and stresses, with a relative error factor of 1:100:100. We split training and validation sets in a ratio of 9:1 (common ratio) and use a batch size of 1. We start with a learning rate (LR) of 10^{-3} and use a LR scheduler that reduces it by half on plateaus with a patience of 50 epochs, stopping the training when the LR is smaller than 10^{-5} . In the following, we refer to these models generically as “Allegro MLIPs”.

C. On-the-fly training sets

In this minimalist approach we limit the number of training runs. Specifically, for BaTiO_3 we only train once, starting from the ferroelectric $R3m$ ground state of the material. For both BiFeO_3 and PbZrO_3 , we train first starting from the $R3c$ ferroelectric polymorph (which is the ground state for BiFeO_3), and then we expand the training set via a second MD run starting from the $Pnma$ non-polar polymorph.^{41,45} Finally, for HfO_2 we train first starting from the $P2_1/c$ non-polar monoclinic ground state, to then extend the training set with a second MD run starting from another non-polar polymorph with tetragonal symmetry $P4_2/nmc$. For the perovskites (BaTiO_3 , BiFeO_3 , and PbZrO_3) we always train using a 40-atom supercell that can be viewed as a $2 \times 2 \times 2$ multiple of the elemental 5-atom perovskite cell. Note that, in particular, this implies that the training for PbZrO_3 never explores the lowest-energy antiferroelectric and ferrielectric polymorphs of the material.⁴² For HfO_2 , we train using a 24-atom that can be seen as obtained from the primitive cell of the tetragonal polymorph by applying a transformation that doubles the volume while keeping the cell as isotropic as possible.

In Fig. 1 we illustrate two methods to track the explored space during the training. For perovskites, since we are training in the 40-atom unit cell, we can extract the amplitude of the main distortions that characterize the structures, namely the polarization (P) and the in-phase (M) and antiphase (R) tilts of the O_6 octahedra. In the top panels of Fig. 1 we show the histogram of occurrences of these distortion along the training trajectory for BiFeO_3 starting from the $R3c$ phase. We can see thermal activation makes the system fluctuate around the ground state. For HfO_2 , the structural complexity makes it all but impossible to work with a reduced number of key distortions. Instead, as shown in the bottom panel of Fig. 1, we compute the powder diffraction spectrum (using the visualization software VESTA⁴⁶) of snapshots taken from the training MD trajectory and compare them to the result for well-known polymorphs, namely non-polar cubic, tetragonal, and monoclinic as well as the polar orthorhombic phase (oIII). This MD trajectory corresponds to the second stage of our HfO_2 training, which starts from the tetragonal phase with no diffraction peaks present below 30 degrees. However, midway through the training, low-angle peaks appear at around 18 and 25 degrees. These peaks can correspond to either the oIII or the monoclinic phase – however, the characteristic monoclinic peak below 30 degrees is missing, confirming the spontaneous occurrence of the oIII phase in the MD trajectory.

The training sets thus generated contain the following number of structures for which a DFT calculation was performed: 247 for BaTiO_3 , 488 for BiFeO_3 , 1300 for PbZrO_3 , and 463 for HfO_2 . Let us stress that these are very small numbers, as typical ML models in the literature rely on training sets at least 10-times bigger.

Representative examples are the deep neural networks recently proposed for PbZrO_3 in Ref. 47 (based on over 12500 structures and a very carefully curated exploration of the energy landscape, probably including supercells of up to 80 atoms) or for HfO_2 in Ref. 48 (96-atom supercell, 21500 structures). Naturally, we do not claim here that our minimal models will be as accurate or complete as the mentioned potentials. Yet, as we will show, it is worth examining how useful they may be.

D. Details of the first-principles calculations

All first-principles calculations were performed using the projector augmented-wave (PAW) method⁴⁹ as implemented in VASP,^{35,36} with the PBEsol exchange-correlation functional.⁵⁰ We solve explicitly for 6 electrons of O ($2s^2 p^4$), 10 of Ba ($5s^2 p^6 6s^2$), 12 of Ti ($3s^2 p^6 4s^2 3d^2$), 15 of Bi ($5d^{10} 6s^2 6p^3$), 14 of Fe ($3p^6 3d^7 4s^1$), 14 of Pb ($5d^{10} 6s^2 p^4$), 12 of Zr ($4s^2 p^6 5s^2 4d^2$) and 10 of Hf ($5p^6 5d^3 6s^1$). The plane-wave energy cutoff was set to 500 eV in all cases. For Brillouin zone integrations corresponding to the 40-atom cell in our perovskite simulations, we use a Γ -centered $3 \times 3 \times 3$ k -point mesh for BaTiO_3 and PbZrO_3 , and a $2 \times 2 \times 2$ mesh for BiFeO_3 . For HfO_2 , we use a grid of $3 \times 3 \times 3$ k -points for the simulations of the considered 24-atom supercell. For BiFeO_3 , we add a Hubbard U correction of 4 eV for a better treatment of iron's $3d$ electrons.⁵¹

III. RESULTS

We now present our minimalist MLIPs and test their performance. We start by considering how well the models describe configurations that appear during the first-principles MD runs used to derive the corresponding training sets. We thus examine the models' ability to interpolate between structures typical of the explored space, where they are expected to perform very well. Then, we run extrapolation tests designed to push the models outside their comfort zone. Here we look at structures and properties well beyond the training set, including features that are critical in investigations of phase transitions (e.g., dynamic stability of higher-symmetry reference phases, stability and energy of additional polymorphs), non-linear responses to external fields (switching paths and energy barriers), and emerging strongly inhomogeneous orders (nanoscale topological textures). These tests allow us to gauge to what extent the models can generalize and still produce physically meaningful results, even when applied in regimes they were not trained for.

A. Interpolation tests

To quantify our models' accuracy at interpolating inside the training space, we proceed as follows. From each of the MD simulations used to generate training sets on the fly, we extract 1% of the visited structures, equispaced. For each such structure we run a single-point DFT calculation to compute energy, forces, and stresses. We run the same calculations using the corresponding MLIPs and compare their predictions to the DFT results. The histograms of the differences between MLIP predictions and DFT results are shown in Fig. 2.

We find that, across all systems, both our VASP and Allegro models show relatively narrow error distributions, which implies that the MLIPs perform well reproducing DFT results. Most of the predictions fall within ± 5 meV per formula unit (f.u.) for energy, ± 50 meV/ \AA for force components, and ± 3 kBar for stress components. Both models show a broader and noisier error distribution for the energies, suggesting that they are harder to learn. This could be due to the relatively small number of energy data points (1 per configuration in the training set) as compared to forces (tens per configuration) or stresses (6 per configuration). Among the considered materials, the models for HfO_2 seem the most accurate. Overall, while both approaches work well to reproduce our minimal datasets, Allegro seems to offer a small edge in accuracy within the explored configuration space.

B. Extrapolation tests

We perform two kinds of extrapolation tests. First, for all the materials we compute the phonons of a high-symmetry phase that appears as the natural reference from which all the low-energy structures of interest can be obtained through appropriate distortions. This reference phase is the ideal cubic perovskite structure for BaTiO_3 , BiFeO_3 , and PbZrO_3 , and the ideal cubic fluorite structure for HfO_2 . Note that the phonons of such reference structures provide a guide to the symmetry- and energy-lowering distortions of the materials, and are thus critical in the study of phase transitions. (The physical relevance of the cubic fluorite structure to ferroelectric HfO_2 is currently debated,⁵² but considering the phonons of this phase still serves our current testing purposes.)

Second, we perform a battery of material-specific tests. For BaTiO_3 we examine the vortex-antivortex electric dipole texture recently reported in Ref. 39, one of the foundational results of the field of moiré multilayers based on perovskite-oxide membranes. For BiFeO_3 we examine the non-trivial structural transition path associated to the reversal of one polarization component, key to the magnetoelectric switching properties (i.e., electric control of the magnetization) in this material.^{40,53} For PbZrO_3 we inspect the relative stability of low-lying polymorphs of diverse electric character (antiferro, ferro, ferri), critical to the phase transitions and antifer-

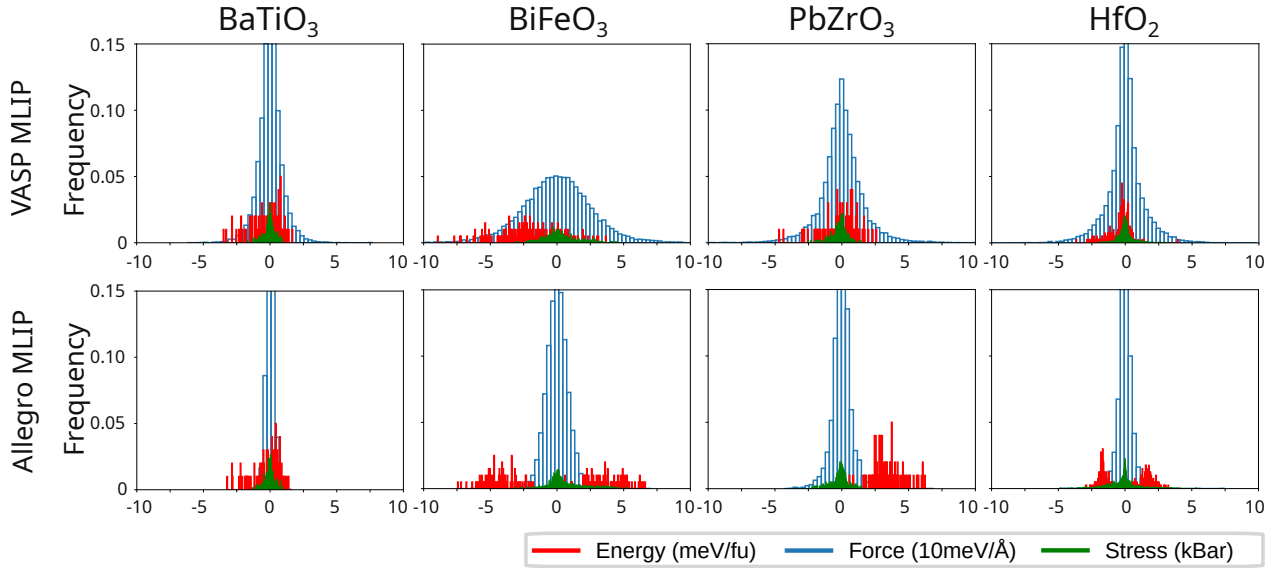


FIG. 2. Histograms for the errors made by our minimalist MLIPs in reproducing the DFT energies, forces, and stresses corresponding to structures typical of the explored configuration space (see text). Each distribution is normalized to 1. We use different bin sizes for clarity.

roelectric response of this compound in bulk and thin-film forms.^{42,54} Finally, for HfO₂ we examine the existence and relative stability of the ferroelectric polymorph that has brought massive interest to this compound, including some of its well-known distinctive features (e.g., the existence of domain walls with a negative formation energy).^{43,52,55,56}

itative errors (fake anomalies) in the response to external fields. This strongly suggests that our minimal MLIPs are both robust and reliable, predicting behaviors that are physically sound even outside the explored training space.

1. Reference-phase phonon bands

We compute the phonons of the cubic phase of each material using DFT and the corresponding MLIP, and compare the results in Fig. 3. (We employ the package phonopy⁵⁷ to compute phonons, using the finite-differences approach in a $2 \times 2 \times 2$ supercell. For the sake of a more direct comparison, we omit non-analytical corrections in these calculations.) Overall, our minimalist MLIPs capture the main features of the phonon spectra remarkably well, reproducing exactly the DFT results for most bands. Notably, all MLIPs correctly predict the main structural instabilities. In BaTiO₃, for example, the models capture the unstable bands with imaginary phonon frequencies (shown as negative frequencies in Fig. 3, following the usual convention). The most notable disagreement is found for BiFeO₃, where the MLIPs do not capture a second unstable phonon at the Γ point; this is a fine detail that does not have – as far as we can tell – any practical consequence.

Remarkably too, our MLIPs do not seem to introduce any unphysical features. Most critically, we find no new unstable modes that could lead to artifacts such as false energy minima (i.e., fake competing polymorphs) or qual-

2. BaTiO₃: Vortex-antivortex electric texture

Bulk barium titanate is paraelectric and cubic above 393 K, approximately.^{58–60} Upon cooling it undergoes a well-known sequence of phase transitions to ferroelectric phases of different symmetry: tetragonal, orthorhombic, and rhombohedral. In ideal bulk-like conditions (i.e., electric short circuit and zero remnant stress), the polar states tend to be homogeneous. Under specific electric or elastic boundary conditions – e.g., as in epitaxial thin films – BaTiO₃ presents multidomain states that essentially follow well-known laws such as Kittel's⁶¹.

Recently, experiments on twisted freestanding bilayers of BaTiO₃ have revealed a mesmerizing and unprecedented type of ferroelectric multidomain configuration: a lattice of electric vortices and antivortices that appears at the interface between layers³⁹, essentially as shown in Fig. 4. Costly DFT calculations helped ascertain the origin of such dipole texture: the shear-strain modulation induced by the moiré interfacial potential gives rise to the observed vortical pattern through the flexoelectric effect, i.e., the polar response to strain gradients.⁶² The DFT analysis concluded that the vortex-antivortex dipole lattice lies about 9 meV/f.u. above an homogeneous state with a net polarization along a $\langle 110 \rangle$ in-plane pseudocubic direction. The simulations relied on drastic simplifi-

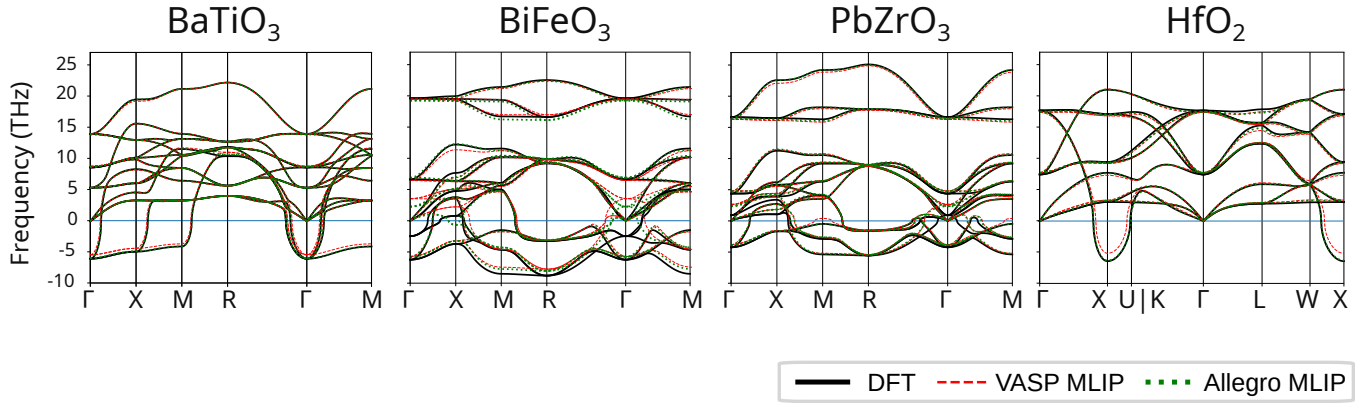


FIG. 3. Phonon bands for high-symmetry reference phases (see text). In black, solid lines, the DFT result. In red, long dashed lines, the VASP MLIP prediction. In green, short dashed lines the Allegro MLIP prediction.

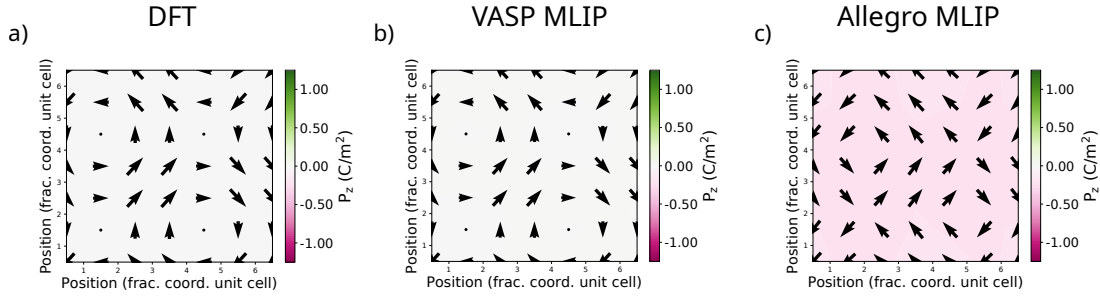


FIG. 4. Vortex-antivortex electric dipole patterns mimicking experimental observations in BaTiO₃ moiré bilayers (see text). The arrows denote in-plane local polarization components (see text), while the color map corresponds to the out-of-plane component.

cations – e.g., a bulk-like version of the vortex-antivortex lattice was considered, instead of the actual moiré bilayer. Nevertheless, the connection between polar texture and inhomogeneous strain was clearly established, evidencing a key role of the flexoelectric effect that was corroborated by other authors shortly after^{63,64}.

The mentioned vortex-antivortex lattice displays many non-trivial features that provide a stringent test to the predictive power of our minimalist MLIPs for BaTiO₃. Most notably, it displays strong polarization gradients and a giant density of non-trivial ferroelectric domain walls. Additionally, the flexoelectric connection between polarization and strain gradients is non-trivial in itself, as it reflects subtle electromechanical couplings, strictly in the long wavelength limit ($\mathbf{q} \rightarrow \mathbf{0}$).⁶⁵ All these are features that our simple MLIPs for BaTiO₃ (trained on DFT data obtained from small 40-atom cells) cannot be expected to capture accurately, in principle. At the same time, our models do contain information about the (short-range) interatomic couplings that are expected to dominate the energetics of domain walls in these materials. (See the Discussion section for a comment on long-range electrostatic couplings.) Hence, one may wonder: is that information enough to predict, at a qualita-

tive level at least, the occurrence and main features of the vortex-antivortex pattern of Fig. 4 as obtained from DFT?

We tested our MLIPs by relaxing the vortex-antivortex structures that some of us studied in Ref. 39 using DFT. The basic results of this exercise are captured in Fig. 4, which shows the electric dipoles extracted from the atomic structure following the same procedure as in Ref. 39. (In essence, we plot Ti-centered electric dipoles, computed for each Ti cation in the lattice.) Remarkably, both MLIPs relax to local energy minima that retain the vortex-antivortex texture obtained in DFT and observed experimentally. The agreement between the structures obtained with DFT and the VASP MLIP is nearly perfect; the Allegro model, on the other hand, predicts correctly the magnitude of the local dipoles but fails to capture the size of the vortex and antivortex cores. A clear connection between electric texture and local strain is established in all cases (not shown here). Finally, the energy difference between the textured state and the competing homogeneous solution with polarization in-plane is 10 meV/f.u. and 1 meV/f.u., respectively, for the VASP and Allegro MLIP, both remarkably close to the DFT value of 9 meV/f.u.

In conclusion, our minimal MLIPs for BaTiO₃ perform very well when applied to a problem that clearly lies beyond the training space explored in the model construction. There is no doubt that these MLIPs could have been used to reach the basic conclusions of the DFT analysis in Ref. 39, namely, the existence of low-lying local energy minima featuring a lattice of electric vortices and antivortices, and the connection between such a dipole pattern and the spatial modulation of shear strains. The difference: a 10⁴-fold speed up in the corresponding simulations, from weeks to minutes of CPU time.

3. BiFeO₃: Switching path

So far, BiFeO₃ is the only room-temperature magnetoelectric multiferroic material of practical importance.⁶⁶ Its remanent polarization has been experimentally measured to be one of the largest among ferroelectrics, with $P \approx 1 \text{ C/m}^2$, while the typical coercive field is also relatively large (around 200 kV/cm for bulky samples). Room-temperature electric control of magnetization was demonstrated in BiFeO₃ already in 2014.⁴⁰ To advance toward a technological use of such a magnetoelectric switching effect, several outstanding issues remain, including a needed reduction in the coercive field so that ultralow-power actuation can be achieved. A significant research effort focuses on this goal.^{67,68}

In this context, there is interest in studying switching barriers and paths in BiFeO₃, which can be estimated from DFT, e.g. by using the so-called “nudged elastic band” method.⁶⁹ Critically, both the switching barrier and the corresponding structural path need to be optimized in order to achieve ultralow-power magnetoelectric switching in BiFeO₃. Specifically, it is important to work in conditions such that polarization switching is accompanied by a reversal of the antiphase octahedral tilts characteristic of BiFeO₃’s ferroelectric phase, as the latter control the sign of the magnetization.^{40,70,71}

Hence, to test our BiFeO₃ models, we compute the switching path corresponding to the reversal of one polarization component, which captures the main features of the effect. Figure 5 shows the comparison between DFT and MLIP results. The MLIPs predict almost exactly the energy barrier and corresponding distortions, including the sign reversal of the R_z component of the antiphase O₆ tilts. Bear in mind that the switching proceeds through a transition state, with $P_z = R_z = 0$ that is never explored in the training (see Fig. 1). Yet, the DFT energy barrier is reproduced within 1 meV/f.u.

4. PbZrO₃: discovering unprecedented phases

PbZrO₃ may well be the inorganic perovskite with the richest low-energy landscape.^{41,42,47,72} Experimentally, the bulk stable phase at ambient conditions is anti-ferroelectric (AFE₄₀ in the following). It features oxy-

TABLE I. Comparison of DFT and MLIP energies for the four low-energy phases of PbZrO₃ considered (see text). Energies are given in meV/f.u. The AFE₄₀ phase is taken as the zero of energy.

	DFT	VASP MLIP	Allegro MLIP
FiE	-0.84	-2.04	-3.80
AFE ₈₀	-0.89	-4.66	-1.78
AFE ₄₀	0.00	0.00	0.00
FE	+0.23	-11.12	-13.11
Cubic	278	272	261

gen octahedral rotations, antiparallel displacements of the Pb cations, and significantly deformed O₆ groups. A rhombohedral ferroelectric phase (FE) with $R\bar{3}c$ symmetry is very close in energy and generally assumed to be the structure the material adopts upon application of an electric field. Then, recent calculations by some of us predicted that a ferrielectric phase (FiE), with uncompensated antiparallel displacements of the Pb atoms, has a lower energy than the AFE₄₀ polymorph. Further, it has been shown from first principles that the AFE₄₀ phase itself presents a cell-doubling instability, yielding yet another low-energy structure (AFE₈₀).^{42,72} Strikingly, DFT predicts that these four phases lie within a 1 meV/f.u. energy window⁴², which poses a challenge for effective modeling.

Table I shows our results for the energies of PbZrO₃’s main competing polymorphs. (The MLIP-obtained lattice parameters and atomic structures are virtually identical to the DFT results, with deviations of 1 % at most, and are not shown here.) Most remarkably, our MLIPs correctly predict the existence of the AFE₄₀, AFE₈₀, and FiE phases. Further, these polymorphs are found to lie within a few meV per formula unit of each other, essentially capturing the near-degeneracy obtained from DFT. Table I also shows that our minimal MLIPs are not perfect, though, as they exaggerate the stability of the FE polymorph. Further, the energy gap between the cubic perovskite structure and the low-energy polymorphs is severely underestimated.

To see this result in its appropriate context, note that our MLIPs for PbZrO₃ are constructed based on knowledge about common and simple perovskites, i.e., phases displaying standard polar distortions and “Glazer patterns” of perfect in-phase and antiphase O₆ octahedral tilts.⁷³ Our exercise shows that such MLIPs would have allowed us to discover exceedingly rare and non-trivial new phases, such as the mentioned AFE₄₀, AFE₈₀, and FiE structures, that are nowhere to be found in the data used to construct the models. More specifically, our MD simulations explore distorted low-energy configurations that lie far – both structure and energy wise – from the perfect cubic structure. More critically, our minimal training set is derived from DFT simulations using a 40-atom supercell that can be seen as a $2 \times 2 \times 2$ repetition of the elemental 5-atom perovskite unit, which is incom-

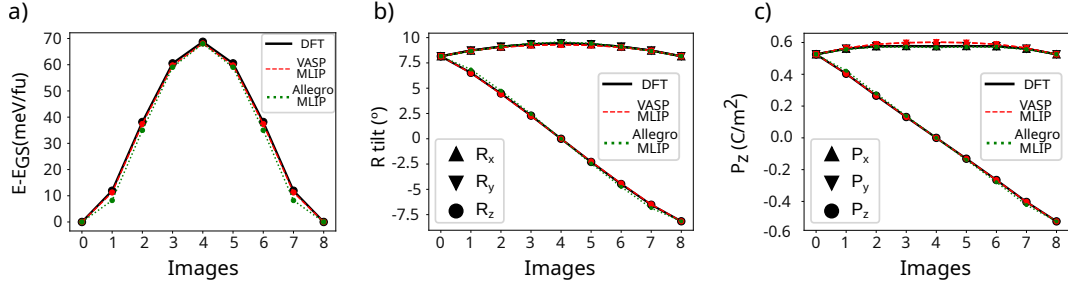


FIG. 5. Ferroelectric switching path for BiFeO_3 (see text). Shown are, as a function of structure along the path, the energy vs polarization (a), polarization components (b), and antiphase tilt components (c).

TABLE II. Comparison of DFT and MLIP energies for the key polymorphs of HfO_2 considered (see text). Energies are given in meV/f.u. The monoclinic phase is taken as the zero of energy.

	PBEsol	VASP MLIP	Allegro MLIP
monoclinic	0	0	0
tetragonal	139	140	143
oIII	64	65	67
oI	16	14	60
cubic	207	188	208

patible with any of the AFE and FiE polymorphs that attract so much attention today. Nevertheless: Based on the MLIP predictions, we could then refine the models through further training on the new polymorphs, so that, for example, the energy gap with the FE structure in Table I be corrected.

Our PbZrO_3 example thus suggests that MLIPs provide us with a platform for materials discovery studies, starting with minimal models that can eventually be improved based on the most surprising predictions coming from the models themselves.

5. HfO_2 : polymorphism and ferroelectricity

Of the ferroelectric oxides in this study, HfO_2 can be considered the odd one out. Prior to the discovery of its polar phase in 2011,⁴³ HfO_2 was already industrially relevant, in use as a high-k gate dielectric in field-effect transistors. Consequently, the observation of ferroelectricity in ultrathin films immediately drew enormous interest. Several MLIP studies of HfO_2 and the closely related fluorite ZrO_2 have been reported, typically based on deep neural network potentials.⁴⁸ Applications of such MLIPs include studies of oxygen mobility,⁷⁴ piezo- and pyroelectric responses,⁷⁵ or the mechanism of antiferroelectricity in ZrO_2 .⁷⁶

Within our minimalist approach, we aim at (re)discovering the most common ferroelectric phase

of HfO_2 (usually denoted “oIII”, with orthorhombic symmetry $Pca2_1$). We also examine whether our models predict the correct hierarchy between competing polar and non-polar polymorphs. Our results are summarized in Table II. (We only provide energies in this Table, as the MLIP-predicted structures match the DFT results to within 1% for all considered phases.) Remarkably, our MLIPs yield a stable oIII polymorph with nearly perfect energy as compared to the DFT result. The excellent accuracy in the oIII prediction can be attributed to the fact that our MD runs find this state serendipitously (see Section II and Fig. 1), so it is in fact included in the training data. More surprising is the fact that both MLIPs reproduce correctly the ordering, energy wise, of all the polymorphs considered. While we find some significant quantitative deviations – as e.g. in the VASP-MLIP result for the cubic phase, or the Allegro-MLIP result for the oI polymorph – those were to be expected, as the cubic and oI states are nowhere to be found in the training space.

It is also worth noting that an even simpler MLIP (trained on DFT data for 12-atom cells, and comprising only 63 DFT calculations) is already capable of predicting the oIII local minimum with near-DFT accuracy in what regards the structure and a remarkably solid value for the energy (42 meV/f.u. above the monoclinic ground state vs. 64 meV/f.u. from DFT). Another unique feature of oIII hafnia is that it features a negative energy of its 180° ferroelectric domain walls. This striking result stems from the fact that the antipolar oI state (which can be viewed as a ferroelectric multidomain configuration) lies below the oIII structure, a property predicted by our MLIPs.

IV. DISCUSSION

Our results carry some implications – both general and specific to ferroelectrics – that merit a brief comment.

This study provides evidence for how relatively simple models can reliably predict phenomena outside their theoretical application scope. Hence, our results can be

viewed in the context of a broader theme: how increasing model complexity can degrade predictive power outside the training range.^{77,78} In the future, it would be interesting – and potentially rewarding – to explore how recent “domain generalization” approaches perform in materials-science problems, e.g. those involving the family of ferroelectric materials considered here. Conversely, it may be valuable to examine whether domain expertise in ferroelectrics and related condensed-matter fields could help define testbeds where the predictive power of general ML schemes can be evaluated, thereby contributing to the development of smarter and more efficient general-purpose algorithms.

Along the same lines, our results suggest that it would be worthwhile to conduct a more systematic investigation into how, and under what circumstances, excessive training of ML models – such as general neural networks – may lead to reduced predictive power outside the training space. Likewise, our findings motivate further studies on the predictive performance of MLIPs even simpler than those considered here; for example, families of interpretable potentials based on physically motivated functional forms.^{4,6} In our view, striking the right balance between accuracy and predictive power will be essential for establishing practical usage guidelines for MLIPs and developing protocols tailored to the goals of specific investigations. MLIPs offer almost unlimited flexibility in model choice for particular applications, and making informed decisions on how to proceed in each case may increasingly become the distinctive human contribution to this field. Achieving that will require systematic studies that build upon the somewhat anecdotal – though, in our view, very compelling – evidence provided by works such as the present one.

When it comes to the particular case of the ferroelectrics investigated in this work, we should first stress that the incredible predictions reported here are a testimony to the value of the employed MLIP and on-the-fly learning schemes,^{1,3,5,37,38,44} which enable the construction of incredibly useful models based on a very modest amount of DFT simulations. This is remarkable particularly when it comes to neural network potentials, commonly believed to be exceedingly data hungry.

It is also worth noting that this project began as a test of a very specific hypothesis. We believed that kernel-based GAP-SOAP MLIPs should be able to capture the dominant short-range interactions in ferroelectric oxides from a modest amount of training data. In particular, we aimed to explore the feasibility of using very small simulation supercells for training. Our intuition was based on earlier work with second-principles potentials,^{16,26} which showed that DFT data from small supercells is sufficient to characterize the interatomic interactions underlying remarkably complex structural phenomena – such as the electric skyrmions predicted (and later experimentally confirmed) in perovskite ferroelectrics.^{32,33,79} The present study confirms that initial hypothesis and, more unexpectedly, indicates that our intuition extends to cu-

rated neural-network frameworks such as Allegro. Ultimately, we think this serves as an example of how a physics-based expectation – namely, that relatively simple short-ranged couplings can produce great complexity, yet remain easy to learn and model – can guide the identification of promising strategies for using MLIPs.

As a final note, long-range Coulomb interactions between electric dipoles are known to play a major role in the physics of ferroelectrics, as e.g. they create depolarizing fields that are one of the main factors leading to the formation of complex multidomain structures. Traditionally, effective atomistic potentials of ferroelectrics have treated such dipole-dipole interactions exactly, using their well-known analytic form and evaluating them via Ewald sums.^{16,21,80} The difficulties to include such interactions within MLIP schemes was a blocking point for the widespread adoption of the new models in the ferroelectrics community.⁸¹ Nevertheless, growing evidence suggest that MLIPs including mid-ranged interactions (e.g., within 5 Å to 8 Å, as done here) are able to effectively capture all relevant couplings, and that a careful treatment of the long-range Coulomb coupling is only needed to address very specific features (e.g., for a correct quantitative treatment of non-analytical properties such as the longitudinal-transversal optical frequency splitting).^{82–84} The present results further support this conclusion and the usefulness of short-ranged MLIPs to study complex ferroelectric phenomena.

V. SUMMARY AND CONCLUSIONS

In this work we examine the performance of machine-learned interatomic potentials (MLIPs) in predicting intricate structural (and, to some extent, functional) properties of representative ferroelectric and related materials. We work with standard and widely-available kernel-based models, as well as with neural network models derived from the same training sets. We restrict ourselves to small training sets generated on-the-fly and without any fine tuning. We also adopt modest unoptimized choices of the MLIP-defining hyperparameters. Then, we test the predictive performance of the resulting minimalist MLIPs.

Within the explored parameter space, both types of MLIPs reproduce DFT energies, forces, and stresses with good fidelity. More notably, the models extrapolate in a physically meaningful way beyond the training space, correctly predicting critical, previously unexpected properties of these compounds – from the emergence of novel polymorphs and topological states to the occurrence of complex polarization switching paths. The success of these minimalist MLIPs challenges the prevailing view that reliable potentials necessarily require large, curated datasets and extensive optimization. Rather, our results show that simple, low-cost and low-knowledge training strategies can yield models capable of unveiling unprecedented non-trivial behaviors. If this is true for materials

as complex – structurally and lattice-dynamically – as the considered ferroelectric oxides, it is essentially guaranteed that our conclusions will pertain to many other materials families as well.

Our results also suggest that complex structural problems such as those considered here could serve as valuable testbeds for domain-generalization approaches currently being explored in the context of general machine learning. Our work also opens promising avenues for investigating the use of simple MLIPs in exploratory research explicitly aimed at uncovering novel “out-of-scope” phenomena. We thus hope that the present work will contribute

to a more informed and effective use of ML methods, broadening their role from tools of interpolation to practical instruments for discovering and predicting emergent physical behavior.

Fruitful discussions with N. Bristowe (Durham) are gratefully acknowledged. Work supported by the Luxembourg National Research Fundt through grants BRIDGES/18421428/SWITCHON (I.R.-M. and J.Í.-G., co-funded by Intel Corporation), INTER/NSF/24/18804122/PIEZOHAFNIA (B.M. and J.Í.-G.), and C23/MS/17909853/BUBBLACED (J.Í.-G. and H.A.).

-
- ¹ Albert P. Bartók and Gábor Csányi, “Gaussian approximation potentials: A brief tutorial introduction,” International Journal of Quantum Chemistry **115**, 1051–1057 (2015).
- ² Han Wang, Linfeng Zhang, Jiequn Han, and Weinan E, “DeePMD-kit: A deep learning package for many-body potential energy representation and molecular dynamics,” Computer Physics Communications **228**, 178–184 (2018).
- ³ Ryosuke Jinnouchi, Ferenc Karsai, and Georg Kresse, “On-the-fly machine learning force field generation: Application to melting points,” Phys. Rev. B **100**, 014105 (2019).
- ⁴ Zheyong Fan, Zezhu Zeng, Cunzhi Zhang, Yanzhou Wang, Keke Song, Haikuan Dong, Yue Chen, and Tapio Ala-Nissila, “Neuroevolution machine learning potentials: Combining high accuracy and low cost in atomistic simulations and application to heat transport,” Physical Review B **104**, 104309 (2021).
- ⁵ Albert Musaelian, Simon Batzner, Anders Johansson, Lixin Sun, Cameron J. Owen, Mordechai Kornbluth, and Boris Kozinsky, “Learning local equivariant representations for large-scale atomistic dynamics,” Nature Communications **14**, 579 (2023).
- ⁶ Stephen R. Xie, Matthias Rupp, and Richard G. Hennig, “Ultra-fast interpretable machine-learning potentials,” npj Computational Materials **9**, 162 (2023).
- ⁷ Ilyes Batatia, Philipp Benner, Yuan Chiang, Alin M. Elena, Dávid P. Kovács, Janosh Riebesell, Xavier R. Advinula, Mark Asta, Matthew Avaylon, William J. Baldwin, Fabian Berger, Noam Bernstein, Arghya Bhowmik, Samuel M. Blau, Vlad Cărare, James P. Darby, Sandip De, Flaviano Della Pia, Volker L. Deringer, Rokas Elijošius, Zakariya El-Machachi, Fabio Falcioni, Edvin Fako, Andrea C. Ferrari, Annalena Genreith-Schriever, Janine George, Rhys E. A. Goodall, Clare P. Grey, Petr Grigorev, Shuang Han, Will Handley, Hendrik H. Heenen, Kersti Hermansson, Christian Holm, Jad Jaffar, Stephan Hofmann, Konstantin S. Jakob, Hyunwook Jung, Venkat Kapil, Aaron D. Kaplan, Nima Karimtari, James R. Kermode, Namu Kroupa, Jolla Kullgren, Matthew C. Kuner, Domantas Kuryla, Guoda Liepuoniute, Johannes T. Margraf, Ioan-Bogdan Magdău, Angelos Michaelides, J. Harry Moore, Aakash A. Naik, Samuel P. Niblett, Sam Walton Norwood, Niamh O’Neill, Christoph Ortner, Kristin A. Persson, Karsten Reuter, Andrew S. Rosen, Lars L. Schaaf, Christoph Schran, Benjamin X. Shi, Eric Sivonxay, Tamás K. Stenczel, Viktor Svahn, Christopher Sutton, Thomas D. Swinburne, Jules Tilly, Cas van der Oord, Eszter Varga-Umbrich, Tejs Vegge, Martin Vondrák, Yangshuai Wang, William C. Witt, Fabian Zills, and Gábor Csányi, “A foundation model for atomistic materials chemistry,” arXiv.2401.00096 (2024), 10.48550/arXiv.2401.00096.
- ⁸ Ryan Jacobs, Dane Morgan, Siamak Attarian, Jun Meng, Chen Shen, Zhenghao Wu, Clare Yijia Xie, Julia H. Yang, Nongnuch Artrith, Ben Blaiszik, Gerbrand Ceder, Kamal Choudhary, Gabor Csanyi, Ekin Dogus Cubuk, Bowen Deng, Ralf Drautz, Xiang Fu, Jonathan Godwin, Vasant Honavar, Olexandr Isayev, Anders Johansson, Boris Kozinsky, Stefano Martiniani, Shyue Ping Ong, Igor Poltavsky, KJ Schmidt, So Takamoto, Aidan P. Thompson, Julia Westermayr, and Brandon M. Wood, “A practical guide to machine learning interatomic potentials – Status and future,” Current Opinion in Solid State and Materials Science **35**, 101214 (2025).
- ⁹ Karin M. Rabe, Charles H. Ahn, and Jean-Marc Triscone, eds., *Physics of Ferroelectrics: A Modern Perspective* (Springer Berlin Heidelberg, Berlin, Heidelberg, 2007).
- ¹⁰ Dennis Meier, Jan Seidel, Marty Gregg, and Ramamoorthy Ramesh, *Domain Walls: From Fundamental Properties to Nanotechnology Concepts* (Oxford University Press, 2020).
- ¹¹ Javier Junquera, Yousra Nahas, Sergei Prokhorenko, Laurent Bellaiche, Jorge Íñiguez, Darrell G. Schlom, Long-Qing Chen, Sayeef Salahuddin, David A. Muller, Lane W. Martin, and R. Ramesh, “Topological phases in polar oxide nanostructures,” Rev. Mod. Phys. **95**, 025001 (2023).
- ¹² Uwe Schroeder, Cheol Seong Hwang, and Hiroshi Funakubo, eds., *Ferroelectricity in doped hafnium oxide: materials, properties and devices*, 2nd ed. (Woodhead Publishing, 2025).
- ¹³ P. Hohenberg and W. Kohn, “Inhomogeneous electron gas,” Physical Review **136**, B864 (1964).
- ¹⁴ W. Kohn and L. J. Sham, “Self-consistent equations including exchange and correlation effects,” Physical Review **140**, A1133 (1965).
- ¹⁵ R. M. Martin, *Electronic Structure: Basic Theory and Practical Methods* (Cambridge University Press, 2004).
- ¹⁶ Jacek C Wojdel, Patrick Hermet, Mathias P Ljungberg, Philippe Ghosez, and Jorge Íñiguez, “First-principles model potentials for lattice-dynamical studies: general methodology and example of application to ferroic per-

- ovskite oxides,” *Journal of Physics: Condensed Matter* **25**, 305401 (2013).
- ¹⁷ Carlos Escorihuela-Sayalero, Jacek C. Wojdeł, and Jorge Íñiguez, “Efficient systematic scheme to construct second-principles lattice dynamical models,” *Phys. Rev. B* **95**, 094115 (2017).
- ¹⁸ Pablo García-Fernández, Jacek C Wojdeł, Jorge Íñiguez, and Javier Junquera, “Second-principles method for materials simulations including electron and lattice degrees of freedom,” *Physical Review B* **93**, 195137 (2016).
- ¹⁹ Nayara Carral-Sainz, Toraya Fernández-Ruiz, Jorge Íñiguez-González, Javier Junquera, and Pablo García-Fernández, “Systematic generation of electron models for second-principles density functional theory methods,” *Physical Review B* **112**, 155146 (2025).
- ²⁰ W. Zhong, David Vanderbilt, and K. M. Rabe, “Phase transitions in BaTiO₃ from first principles,” *Physical Review Letters* **73**, 1861 (1994).
- ²¹ W. Zhong, David Vanderbilt, and K. M. Rabe, “First-principles theory of ferroelectric phase transitions for perovskites: The case of BaTiO₃,” *Physical Review B* **52**, 6301 (1995).
- ²² U. V. Waghmare and K. M. Rabe, “Ab initio statistical mechanics of the ferroelectric phase transition in PbTiO₃,” *Physical Review B* **55**, 6161 (1997).
- ²³ Henry Krakauer, Rici Yu, Cheng-Zhang Wang, Karin M Rabe, and Umesh V. Waghmare, “Dynamic local distortions in KNbO₃,” *Journal of Physics: Condensed Matter* **11**, 3779–3787 (1999).
- ²⁴ L. Bellaiche, Alberto García, and David Vanderbilt, “Finite-temperature properties of Pb(Zr_{1-x}Ti_x)O₃ alloys from first principles,” *Physical Review Letters* **84**, 5427 (2000).
- ²⁵ Sergey Prosandeev, Dawei Wang, Wei Ren, Jorge Íñiguez, and Laurent Bellaiche, “Novel nanoscale twinned phases in perovskite oxides,” *Advanced Functional Materials* **23**, 234–240 (2013).
- ²⁶ Pavlo Zubko, Jacek C Wojdeł, Marios Hadjimichael, Stéphanie Fernandez-Pena, Anaïs Sené, Igor Luk'yanchuk, Jean-Marc Triscone, and Jorge Íñiguez, “Negative capacitance in multidomain ferroelectric superlattices,” *Nature* **534**, 524–528 (2016).
- ²⁷ Ian David Brown, “Recent developments in the methods and applications of the bond valence model,” *Chem. Rev.* **109**, 6858–6919 (2009).
- ²⁸ Young-Han Shin, Valentino R. Cooper, Ilya Grinberg, and Andrew M. Rappe, “Development of a bond-valence molecular-dynamics model for complex oxides,” *Physical Review B* **71**, 054104 (2005).
- ²⁹ S. Tinte, M.G. Stachiotti, M. Sepliarsky, R.L. Migoni, and C.O. Rodriguez, “Atomistic modelling of BaTiO₃ based on first-principles calculations,” *Journal of Physics: Condensed Matter* **11**, 9679 (1999).
- ³⁰ Ivan I. Naumov, L. Bellaiche, and Huaxiang Fu, “Unusual phase transitions in ferroelectric nanodisks and nanorods,” *Nature* **432**, 737–740 (2004).
- ³¹ Y. Nahas, S. Prokhorenko, Lydie Louis, Z. Gui, Igor Kornev, and L. Bellaiche, “Discovery of stable skyrmionic state in ferroelectric nanocomposites,” *Nature Communications* **6**, 8542 (2015).
- ³² M. A. Pereira Gonçalves, Carlos Escorihuela-Sayalero, Pablo García-Fernández, Javier Junquera, and Jorge Íñiguez, “Theoretical guidelines to create and tune electric skyrmion bubbles,” *Science Advances* **5**, eaau7023 (2019).
- ³³ S. Das, Y. L. Tang, Z. Hong, M.A.P. Gonçalves, M.R. McCarter, C. Klewe, K.X. Nguyen, F. Gómez-Ortiz, P. Shafer, E. Arenholz, V.A. Stoica, S.-L. Hsu, B. Wang, C. Ophus, J.F. Liu, C.T. Nelson, S. Saremi, B. Prasad, A.B. Mei, D.G. Schlom, J. Íñiguez, P. García-Fernández, D.A. Muller, L.Q. Chen, J. Junquera, Martin L.W., and R. Ramesh, “Observation of room-temperature polar skyrmions,” *Nature* **568**, 368–372 (2019).
- ³⁴ Hugo Aramberri and Jorge Íñiguez-González, “Brownian electric bubble quasiparticles,” *Phys. Rev. Lett.* **132**, 136801 (2024).
- ³⁵ G. Kresse and J. Furthmüller, “Efficient iterative schemes for ab initio total-energy calculations using a plane-wave basis set,” *Physical Review B* **54**, 11169–11186 (1996).
- ³⁶ G. Kresse and D. Joubert, “From ultrasoft pseudopotentials to the projector augmented-wave method,” *Physical Review B* **59**, 1758–1775 (1999).
- ³⁷ Chuin Wei Tan, Marc L. Descoteaux, Mit Kotak, Gabriel de Miranda Nascimento, Séan R. Kavanagh, Laura Zichi, Menghang Wang, Aadit Saluja, Yizhong R. Hu, Tess Smidt, Anders Johansson, William C. Witt, Boris Kozinsky, and Albert Musaelian, “High-performance training and inference for deep equivariant interatomic potentials,” (2025).
- ³⁸ Simon Batzner, Albert Musaelian, Lixin Sun, Mario Geiger, Jonathan P. Mailoa, Mordechai Kornbluth, Nicola Molinari, Tess E. Smidt, and Boris Kozinsky, “E(3)-equivariant graph neural networks for data-efficient and accurate interatomic potentials,” *Nature Communications* **13**, 2453 (2022).
- ³⁹ G. Sánchez-Santolino, V. Rouco, S. Puebla, H. Aramberri, V. Zamora, M. Cabero, F. A. Cuellar, C. Munuera, F. Mompean, M. Garcia-Hernandez, A. Castellanos-Gomez, J. Íñiguez, C. Leon, and J. Santamaría, “A 2d ferroelectric vortex pattern in twisted BaTiO₃ freestanding layers,” *Nature* **626**, 529–534 (2024).
- ⁴⁰ J.T. Heron, J. L. Bosse, Q. He, Y. Gao, M. Trassin, L. Ye, J. D. Clarkson, C. Wang, Jian Liu, S. Salahuddin, D. C. Ralph, D. G. Schlom, J. Íñiguez, Huey, and R. Ramesh, “Deterministic switching of ferromagnetism at room temperature using an electric field,” *Nature* **516**, pages 370–373 (2014).
- ⁴¹ Jorge Íñiguez, Massimiliano Stengel, Sergey Prosandeev, and L. Bellaiche, “First-principles study of the multimode antiferroelectric transition in PbZrO₃,” *Phys. Rev. B* **90**, 220103 (2014).
- ⁴² Hugo Aramberri, Claudio Cazorla, Massimiliano Stengel, and Jorge Íñiguez, “On the possibility that PbZrO₃ not be antiferroelectric,” *npj Computational Materials* **7**, 196 (2021).
- ⁴³ T. S. Böscke, J. Müller, D. Bräuhaus, U. Schröder, and U. Böttger, “Ferroelectricity in hafnium oxide thin films,” *Applied Physics Letters* **99**, 102903 (2011).
- ⁴⁴ Albert P. Bartók, Risi Kondor, and Gábor Csányi, “On representing chemical environments,” *Phys. Rev. B* **87**, 184115 (2013).
- ⁴⁵ Oswaldo Diéguez, O. E. González-Vázquez, Jacek C. Wojdeł, and Jorge Íñiguez, “First-principles predictions of low-energy phases of multiferroic BiFeO₃,” *Physical Review B* **83**, 094105 (2011).
- ⁴⁶ Koichi Momma and Fujio Izumi, “VESTA₃ for three-dimensional visualization of crystal, volumetric and mor-

- phology data," *Journal of Applied Crystallography* **44**, 1272–1276 (2011).
- ⁴⁷ Huazhang Zhang, Hao-Cheng Thong, Louis Bastogne, Churen Gui, Xu He, and Philippe Ghosez, "Finite-temperature properties of the antiferroelectric perovskite pbzro₃ from a deep-learning interatomic potential," *Phys. Rev. B* **110**, 054109 (2024).
- ⁴⁸ Jing Wu, Yuzhi Zhang, Linfeng Zhang, and Shi Liu, "Deep learning of accurate force field of ferroelectric HfO₂," *Phys. Rev. B* **103**, 024108 (2021).
- ⁴⁹ P. E. Blöchl, "Projector augmented-wave method," *Physical Review B* **50**, 17953–17979 (1994).
- ⁵⁰ John P. Perdew, Kieron Burke, and Matthias Ernzerhof, "Generalized gradient approximation made simple," *Physical Review Letters* **77**, 3865 (1996).
- ⁵¹ S. L. Dudarev, G. A. Botton, S. Y. Savrasov, C. J. Humphreys, and A. P. Sutton, "Electron-energy-loss spectra and the structural stability of nickel oxide: An LSDA+U study," *Physical Review B* **57**, 1505–1509 (1998).
- ⁵² Hugo Aramberri and Jorge Íñiguez, "Theoretical approach to ferroelectricity in hafnia and related materials," *Communications Materials* **4**, 95 (2023).
- ⁵³ Natalya S. Fedorova, Dmitri E. Nikonov, John M. Mangeri, Hai Li, Ian A. Young, and Jorge Íñiguez, "Understanding magnetoelectric switching in BiFeO₃ thin films," *Phys. Rev. B* **109**, 085116 (2024).
- ⁵⁴ Krina Parmar, Pauline Dufour, Emma Texier, Cécile Carrétéro, Xiaoyan Li, Florian Godel, Jirka Hlinka, Brahim Dkhil, Daniel Sando, Hugo Aramberri, Jorge Íñiguez-González, Stéphane Fusil, Alexandre Gloter, Thomas Maroutian, and Vincent Garcia, "Establishing a pure antiferroelectric PbZrO₃ phase through tensile epitaxial strain," *Nature Communications* **16** (2025), 10.1038/s41467-025-61867-y.
- ⁵⁵ Hyun-Jae Lee, Minseong Lee, Kyoungjun Lee, Jinhyeong Jo, Hyemi Yang, Yungyeom Kim, Seung Chul Chae, Umesh Waghmare, and Jun Hee Lee, "Scale-free ferroelectricity induced by flat phonon bands in HfO₂," *Science* **369**, 1343–1347 (2020).
- ⁵⁶ Luis Azevedo Antunes, Richard Ganser, Christopher Kuenneth, and Alfred Kersch, "Characteristics of low-energy phases of hafnia and zirconia from density functional theory calculations," *Physica Status Solidi (RRL) – Rapid Research Letters* **16**, 2100636 (2022).
- ⁵⁷ A Togo and I Tanaka, "First principles phonon calculations in materials science," *Scr. Mater.* **108**, 1–5 (2015).
- ⁵⁸ Walter J. Merz, "The dielectric behavior of BaTiO₃ single-domain crystals," *Phys. Rev.* **75**, 687–687 (1949).
- ⁵⁹ Walter J. Merz, "The electric and optical behavior of BaTiO₃ single-domain crystals," *Phys. Rev.* **76**, 1221–1225 (1949).
- ⁶⁰ M. E. Lines and A. M. Glass, *Principles and Applications of Ferroelectrics and Related Materials*, Oxford Classic Texts in the Physical Sciences (Clarendon Press, Oxford, 1977).
- ⁶¹ Charles Kittel, "Theory of the structure of ferromagnetic domains in films and small particles," *Phys. Rev.* **70**, 965–971 (1946).
- ⁶² Pavlo Zubko, Gustau Catalan, and Alexander K. Tagantsev, "Flexoelectric effect in solids," *Annual Review of Materials Research* **43**, 387–421 (2013).
- ⁶³ Naafis Ahnaf Shahed, Kartik Samanta, Mohamed Elekhtiar, Kai Huang, Chang-Beom Eom, Mark S. Rzchowski, Kirill D. Belashchenko, and Evgeny Y. Tsymbal, "Prediction of polarization vortices, charge modulation, flat bands, and moiré magnetism in twisted oxide bilayers," *Phys. Rev. B* **111**, 195420 (2025).
- ⁶⁴ Sergey Prosandeev, Charles Paillard, and L. Bellaiche, "Understanding and controlling dipolar Moiré pattern in ferroelectric perovskite oxide nanolayers," *Phys. Rev. B* **111**, L180103 (2025).
- ⁶⁵ Massimiliano Stengel, "Flexoelectricity from density-functional perturbation theory," *Phys. Rev. B* **88**, 174106 (2013).
- ⁶⁶ Gustau Catalan and James F. Scott, "Physics and applications of bismuth ferrite," *Advanced Materials* **21**, 2463–2485 (2009).
- ⁶⁷ Bhagwati Prasad, Yen-Lin Huang, Rajesh V. Chopdekar, Zuhuang Chen, James Steffes, Sujit Das, Qian Li, Mengmeng Yang, Chia-Ching Lin, Tanay Gosavi, Dmitri E. Nikonov, Zi Qiang Qiu, Lane W. Martin, Bryan D Huey, Ian Young, Jorge Íñiguez, Sasikanth Manipatruni, and Ramamoorthy Ramesh, "Ultralow voltage manipulation of ferromagnetism," *Advanced Materials* **32**, 2001943 (2020).
- ⁶⁸ Yen-Lin Huang, Dmitri Nikonov, Christopher Addiego, Rajesh V. Chopdekar, Bhagwati Prasad, Lei Zhang, Jayotirmoy Chatterjee, Heng-Jui Liu, Alan Farhan, Ying-Hao Chu, Mengmeng Yang, Maya Ramesh, Zi Qiang Qiu, Bryan D. Huey, Chia-Ching Lin, Tanay Gosavi, Jorge Íñiguez, Jeffrey Bokor, Xiaoqing Pan, Ian Young, Lane W. Martin, and Ramamoorthy Ramesh, "Manipulating magnetoelectric energy landscape in multiferroics," *Nature Communications* **11**, 2836 (2020).
- ⁶⁹ Daniel Sheppard, Penghao Xiao, William Chemelewski, Duane D. Johnson, and Graeme Henkelman, "A generalized solid-state nudged elastic band method," *The Journal of Chemical Physics* **136**, 074103 (2012).
- ⁷⁰ Claude Ederer and Nicola A. Spaldin, "Weak ferromagnetism and magnetoelectric coupling in bismuth ferrite," *Physical Review B* **71**, 060401 (2005).
- ⁷¹ D. Rahmedov, Dawei Wang, Jorge Íñiguez, and L. Bellaiche, "Magnetic cycloid of BiFeO₃ from atomistic simulations," *Physical Review Letters* **109**, 037207 (2012).
- ⁷² JS Baker, M Paściak, JK Shenton, P Vales-Castro, B Xu, J Hlinka, P Márton, RG Burkovsky, G Catalan, AM Glazer, *et al.*, "A re-examination of antiferroelectric PbZrO₃ and PbHfO₃: an 80-atom *pnam* structure," arXiv preprint arXiv:2102.08856 (2021).
- ⁷³ A. M. Glazer, "Simple ways of determining perovskite structures," *Acta Crystallographica Section A* **31**, 756–762 (1975).
- ⁷⁴ Liyang Ma, Jing Wu, Tianyuan Zhu, Yiwei Huang, Qiyan Lu, and Shi Liu, "Ultrahigh oxygen ion mobility in ferroelectric hafnia," *Phys. Rev. Lett.* **131**, 256801 (2023).
- ⁷⁵ Richard Ganser, Simon Bongartz, Alexander von Mach, Luis Azevedo Antunes, and Alfred Kersch, "Piezo- and pyroelectricity in zirconia: A study with machine-learned force fields," *Phys. Rev. Appl.* **18**, 054066 (2022).
- ⁷⁶ Richard Ganser, Patrick D. Lomenzo, Liam Collins, Bohan Xu, Luis Azevedo Antunes, Thomas Mikolajick, Uwe Schroeder, and Alfred Kersch, "Mechanism of antiferroelectricity in polycrystalline ZrO₂," *Advanced Functional Materials* **34**, 2405513 (2024).
- ⁷⁷ Preetum Nakkiran, Gal Kaplun, Yamini Bansal, Tristan Yang, Boaz Barak, and Ilya Sutskever, "Deep double de-

- scent: Where bigger models and more data hurt,” (2019), arXiv:1912.02292.
- ⁷⁸ Ishaan Gulrajani and David Lopez-Paz, “In search of lost domain generalization,” (2020), arXiv:2007.01434.
- ⁷⁹ Jacek C Wojdeł and Jorge Íñiguez, “Ferroelectric transitions at ferroelectric domain walls found from first principles,” Physical Review Letters **112**, 247603 (2014).
- ⁸⁰ X. Gonze and C. Lee, “Dynamical matrices, born effective charges, dielectric permittivity tensors, and interatomic force constants from density-functional perturbation theory,” Physical Review B **55**, 10355 (1997).
- ⁸¹ Linfeng Zhang, Han Wang, Maria Carolina Muniz, Athanassios Z. Panagiotopoulos, Roberto Car, and Weinan E, “A deep potential model with long-range electrostatic interactions,” The Journal of Chemical Physics **156**, 124107 (2022).
- ⁸² Jiyuan Yang and Shi Liu, “Topological phase transitions in perovskite superlattices driven by temperature, electric field, and doping,” Phys. Rev. B **110**, 214112 (2024).
- ⁸³ Lorenzo Monacelli and Nicola Marzari, “Electrostatic interactions in atomistic and machine-learned potentials for polar materials,” (2024), arXiv:2412.01642.
- ⁸⁴ Miao Yu, Fernando Gómez-Ortiz, Louis Bastogne, Jin-Zhu Zhao, and Philippe Ghosez, “Role of long-range dipolar interactions in the simulation of the properties of polar crystals using effective atomic potentials,” Phys. Rev. B **112**, 104324 (2025).